Journal of Non-Crystalline Solids 460 (2017) 1–5

Contents lists available at ScienceDirect

Journal of Non-Crystalline Solids

journal homepage: www.elsevier.com/locate/jnoncrysol

Crystallization kinetics of $Cu_{55}Hf_{45}$ glassy alloy

O. Lozada-Flores [a], I.A. Figueroa [a,*], G.A. Lara [a], G. Gonzalez [a], C. Borja-Soto [b], J.A. Verduzco [b]

[a] Instituto de Investigaciones en Materiales, Universidad Nacional Autónoma de México, Circuito exterior, Ciudad Universitaria, Coyoacán, Ciudad de México, Mexico, 04510
[b] Instituto de Investigación en Metalurgia y Materiales, Universidad Michoacana de San Nicolás de Hidalgo (UMSNH), Fco. J. Mújica S/N, Col. Felícitas del Río, Morelia, Mich. 58030, Mexico

ARTICLE INFO

Article history:
Received 22 November 2016
Received in revised form 10 January 2017
Accepted 12 January 2017
Available online 17 January 2017

Keywords:
Crystallization kinetics
Metallic glasses
Differential scanning calorimetry (DSC)
Activation energy

ABSTRACT

The crystallization kinetics of $Cu_{55}Hf_{45}$ glassy alloy were investigated under non-isothermal and isothermal conditions by differential scanning calorimetry. Under non-isothermal analysis the activation energies of glass transition and crystallization, at the onset and the peak crystallization temperatures were determined based on the Kissinger's method, the experimental values obtained were 700.8 ± 20.3 kJ/mol, 469.4 kJ ± 12.7/mol and 444.73 ± 14.2 kJ/mol, respectively. Under isothermal conditions, the crystallization kinetics was calculated by means of Johnson-Melh-Avrami equation and the activation energy was determined by using the Arrhenius equation. The average activation energy was 447.92 ± 16.1 kJ/mol and the average Avrami exponent value was $n = 2.7$, indicating that the crystallization mechanism implies a volume nucleation and two-dimensional growth. The local activation energy decreased as a function of the increment of crystallization volume, as when the crystallization progresses, the energy required for nucleation decreased and the value of activation energy drops.

1. Introduction

Metallic glasses are materials with lack of long-range order in its atomic structure. Since the first report [1], metallic glasses have attracted a considerable amount of interest because their unique combination of structural and functional properties [2–5]. In particular, binary alloys do not follow the empirical rules generally accepted for glass formation [6], and have been recognized as exhibiting only moderate glass formability because the degree of atomic rearrangement required for crystallization is smaller than that for ternary or higher order alloys. Thus, binary alloys generally require higher cooling rates to suppress crystallization. Several binary compositions have been reported as forming metallic glasses [7–9]. For Cu based binary glassy alloys, different studies have been conducted: formation, mechanical properties and thermal stability for $Cu_{60}Zr_{40}$, $Cu_{45}Zr_{55}$, $Cu_{60}Hf_{40}$ and $Cu_{55}Hf_{45}$ [10], Vickers's hardness, Young's modulus, fracture strength and thermal analysis of $Cu_{66}Hf_{34}$ [8], kinetic study of $Cu_{50}Ti_{50}$ amorphous alloy [11], glass forming ability and kinetics by non-isothermal analysis of $Cu_{65}Hf_{45}$ bulk metallic glass [12,13]. More recently, the glass formation, structure and thermal properties in binary $Cu_{100-x}Hf_x$ alloy system (where x = 25–50 at.%) [14], the comparison of bulk was formation between Cu—Hf and Cu-Hf-Al alloys [15] and the elastics properties for $Cu_{64.5}Zr_{35.5}$, $Cu_{90}Zr_{10}$ [16] were reported. However, very few studies have been carried out focusing in the determination of crystallization kinetics parameters by non-isothermal and, especially, by isothermal analysis for binary Cu based glassy alloys [17,18]. In order to provide more information of this important Cu based binary glassy alloy, in the present work, the crystallization kinetics of $Cu_{55}Hf_{45}$ binary glassy alloy were investigated by non-isothermal and isothermal analysis by differential scanning calorimetry (DSC) to measure the kinetics parameters and the crystallization behavior through the Kissinger's method and others [19]. Finally a Johnson-Mehl-Avrami model [20] was applied at isothermal heating in order to understand the thermal stability and nucleation and growth behavior.

2. Experimental procedures

$Cu_{55}Hf_{45}$ alloy ingots were prepared by argon arc melting mixtures of Cu (99.99% pure) and Hf (99.8% pure). The alloy composition represents nominal values but weight losses in melting were negligible (<0.1%). Each alloy ingot was re-melted at least five times to ensure good chemical homogeneity. Ribbon glassy samples were produced by chill-block melt spinning in a sealed He atmosphere at a roll speed of 25 m/s with an injection pressure of 0.4 bar and a nozzle orifice diameter of 0.8 mm. The gap between the crucible and the copper wheel was approximately 5 mm. The crystallization kinetics of the glassy alloy was characterized by continuous heating and isothermal annealing in a TA SDT Q600 calorimeter. Alumina sample holders and a constant flow of high purity Ar was used. In the case of continuous heating, the heating rates used were 5, 10, 20, 30 and 40 K/min. The isothermal crystallization experiments were carried out in the super-cooled liquid region ($\Delta T_x = T_x - T_g$), the glassy samples were first heated at a rate of 20 K/min up to a fixed temperature (between 495 and 520 K), and

* Corresponding author.
E-mail address: iafigueroa@unam.mx (I.A. Figueroa).

http://dx.doi.org/10.1016/j.jnoncrysol.2017.01.021
0022-3093/

then the samples were kept at the annealing temperature for a period of time until the crystallization is completed, after that, the samples were cooled down to room temperature. The DSC measurements were calibrated using a fresh zinc standard, giving an accuracy of ±0.2 K and ±0.02 mW. Structural characterization was examined by X-ray diffraction (XRD) using Co radiation (λ = 1.78897 Å) in a diffractometter SIEMENS-D5000. Each test was repeated three times in order to calculate the experimental error, using the Student's *t* distribution with 95% of confidence.

3. Results and discussion

3.1. Structural characterization of $Cu_{55}Hf_{45}$ metallic glass

The melt spun ribbons cast for the binary alloy showed high metallic lustre. The XRD pattern of the sample consist only of a broad diffused peak in the 2Θ ranging from 36° to 57°, which indicates the formation of fully glassy phase (Fig. 1). Besides, confirming the XRD fully amorphous structure, the ribbons could easily be bent through 180° without fracture. The produced ribbon thickness was 25 μm, corresponding to the roll speed of 25 m/s.

3.2. Non-isothermal crystallization behavior

The crystallization peaks of DSC curves in $Cu_{55}Hf_{45}$ glassy alloy by means of continuous heating are shown in Fig. 2. As mentioned above, the heating rates chosen were 5 K/min, 10 K/min, 20 K/min, 30 K/min and 40 K/min. All DSC curves exhibited a clear glass transition (T_g), followed by an extended super-cooled liquid region (ΔT_x) before the onset of crystallization (T_x) and a single pronounced exothermic peak (peak temperature, T_p), which is associated to the crystallization phenomena. The values of T_g, T_x, and T_p, at different heating rates are listed in Table 1. These values are similar to the previously reported [14]. It can be seen that all the characteristic temperatures of metallic glasses are shifted to higher temperatures with the increase of heating rate, indicating that both the glass transition and crystallization displays a strong dependence on the heating rate during the continuous heating [21, 22]. This is caused by the fact of nucleation is a thermally activated process, while the kinetics behavior of glass transition is due to the relaxation processes in the glass transition region [23].

In Fig. 3, the relationship between the crystallization fraction (α) of the $Cu_{44}Hf_{45}$ glassy alloys as a function of different heating rates is shown. All curves exhibited a sigmoidal dependence with temperature. This behavior is typical in the amorphous materials by isothermal and continuous heating.

The activation energy of glass transition and crystallization for the investigated $Cu_{55}Hf_{45}$ metallic glass has been estimated by means of the Kissinger's method [19], according to the following equation:

$$\mathrm{Ln}\left(\frac{T^2}{\beta}\right) = \frac{E_a}{RT} + C \qquad (1)$$

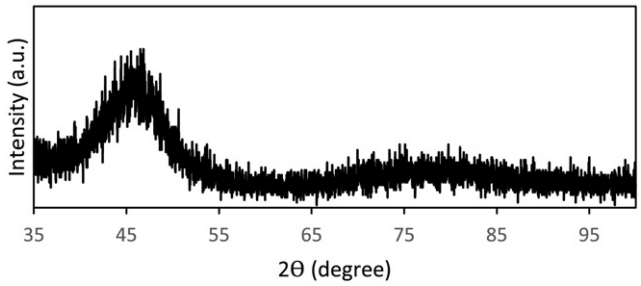

Fig. 1. XRD pattern of the $Cu_{55}Hf_{45}$ glassy alloy ribbon.

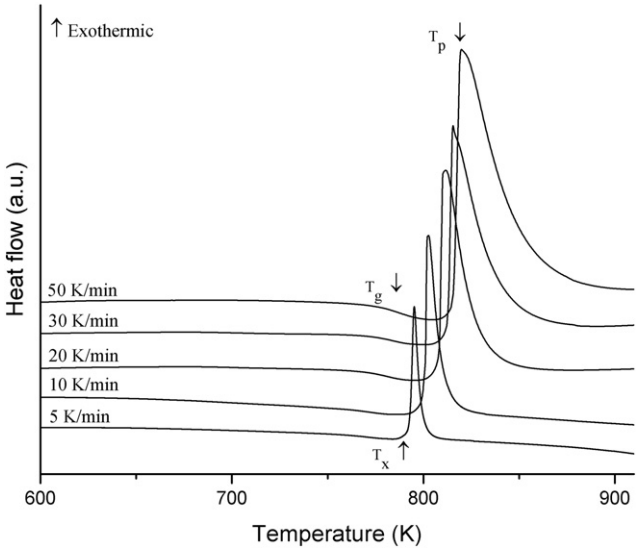

Fig. 2. DSC curves of $Cu_{55}Hf_{45}$ glassy alloy at different heating rates.

where β is the heating rate, R the gas constant and T is the specific temperature (T_g, T_x or T_p), E_a is the effective activation energy for glass transition and crystallization temperatures (T_g, T_x and T_a) and C is a constant. Fig. 4 shows the $Ln(T^2/\beta)$ vs $1000/T$ Kissinger's plot, an approximately straight line with the E/R slope can be obtained, with these values, the activation energy was calculated. The obtained values of E_g, E_x and E_p are 700.8 ± 20.3 kJ/mol, 469.4 kJ ± 12.7/mol and 444.73 ± 14.2 kJ/mol, respectively. The value of E_g is higher than those for E_x and E_p, suggesting that the energy required for glass transition (endothermic process) is greater than the energy required for the crystallization of this glassy alloy (exothermic process) This indicates that the atomic diffusion requires higher amounts of energy through glass transition process (in which the temperature values are lower) than in the crystallization. The E_x values are associated with the nucleation and the E_p values are related to the grain growth [24], therefore, the nucleation process requires higher amount of energy than that for the grain growth process.

3.3. Isothermal crystallization behavior

The isothermal analysis of $Cu_{55}Hf_{45}$ glassy alloy was carried out at different annealing temperatures within the super-cooled liquid region ($\Delta T_x = T_x - T_g$) the selected temperatures were 768, 773, 778, 783, 788 and 793 K. It was observed that each DSC curve presents an incubation time, τ. This time is defined as the time scale between the time reaching the annealing temperature and the start time of crystallization process, followed by a single exothermic peak. The latter is associated to the time interval between the onset of crystallization and the ending crystallization times. Here, if a higher annealing temperature is needed, a lower annealing time will be required. This implies that the crystallization route is via "nucleation and growth" process [25], as can be observed in Fig. 5.

Table 1
Values of T_g, T_x, T_p and ΔT_x of $Cu_{44}Hf_{45}$ glassy alloy ribbon.

Heating rate (K/min)	T_g (K)	T_x (K)	T_p (K)	ΔT_x (K)
5	760 ± 4	793 ± 3	795 ± 2	33 ± 7
10	764 ± 3	801 ± 2	803 ± 2	37 ± 5
20	768 ± 4	808 ± 2	812 ± 3	40 ± 6
30	772 ± 3	813 ± 2	815 ± 1	41 ± 5
40	774 ± 5	816 ± 2	820 ± 2	42 ± 7

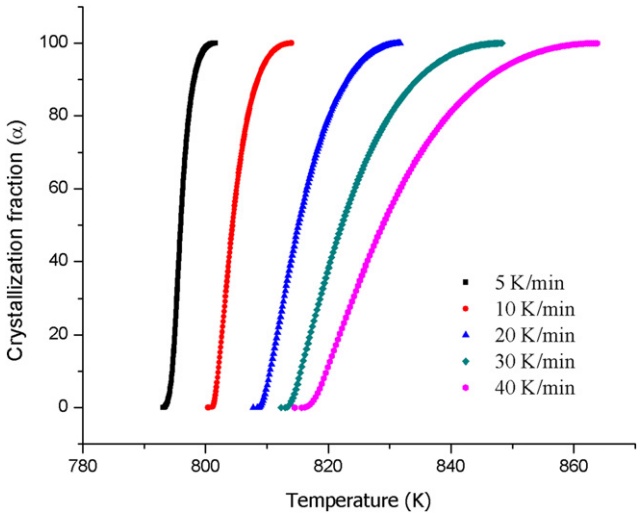

Fig. 3. Relationship between crystallization fraction (α) and temperature, at different heating rates.

The crystallized volume fraction is proportional to the fractional area of exothermic peak and can be expressed as a function of annealing time, according to the following equation [26]:

$$\alpha(t) = \frac{A(t)}{A_\infty} \tag{2}$$

where A_∞ is the total area of the exothermic peak and A(t) is the partial area of exothermic peak between the onset crystallization time and the chosen time. Fig. 6 shows the sigmoidal curves obtained by plotting the crystallization fraction (α) as a function of the annealing time. It can be noted that the crystallization process is much faster when increasing the annealing temperature. This could be related to the annealing temperatures, since at higher annealing temperatures, near to T_x, the atomic mobility is much greater and, therefore, the crystallization occurs almost spontaneously.

The isothermal crystallization kinetics of $Cu_{55}Hf_{45}$ glassy alloy can be modeled by the Johnson-Melh-Avrami equation (JMA) [20,27] as follows:

$$\alpha(t) = 1 - \exp\{-[K(t-\tau)^n]\} \tag{3}$$

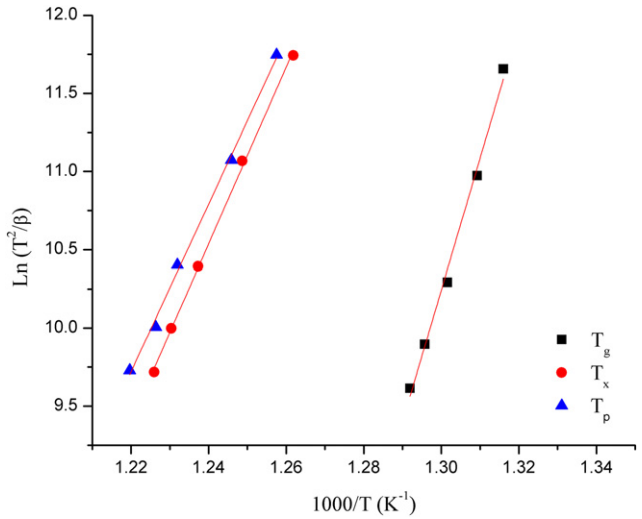

Fig. 4. Kissinger's plots for $Cu_{55}Hf_{45}$ glassy alloy, from which E_g, E_x and E_p are calculated.

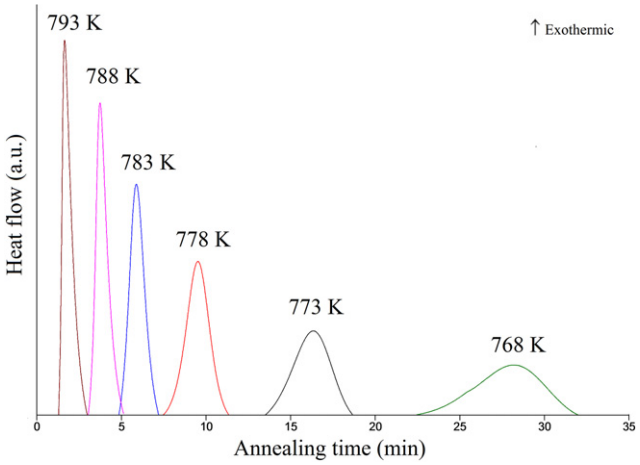

Fig. 5. DSC curves of $Cu_{55}Hf_{45}$ glassy alloy at different annealing temperatures.

where *n* is the Avrami exponent, which is related to the characteristics of nucleation and growth during crystallization, τ is the incubation time and K is a reaction rate constant related to the activation energy for the process. Taking the double logarithm of Eq. (3) the following expression is obtained [28]:

$$\ln[-\ln(1-\alpha(t))] = n\ln K + n\ln(t-\tau) \tag{4}$$

Fig. 7 shows the JMA plots at the chosen annealing temperatures for $0.10 \le \alpha \le 0.90$, the Avrami exponent *n* and the reaction rate constant *K* can be obtained from the slope and intercept of this curves. These results are given in Table 2. It can be noted that the values of *n* (in isothermal analysis), increased from 2.78 to 3.07 for annealing temperatures of 768 K and 778 K, respectively. Then, it decreased down to a value of 1.35 for an annealing temperature of 793 K. This can be attributed to the fact that at lower annealing temperatures (such as 768 K and 773 K) the atomic diffusion is retarded, impacting on the nucleation and growth, and therefore, resulting in a drop in nucleation rate. On the other hand, at 778 K, the mobility of the atoms in ΔT_x is relatively easy, promoting the increment of the nucleation rate. It is known that the values of *n* are related to different crystallization transformation mechanism [29]: for $n \approx 3$ (associated with temperatures near T_g) implies a volume nucleation and two dimensional growth. With $n \approx 1$ (at 793 K), the

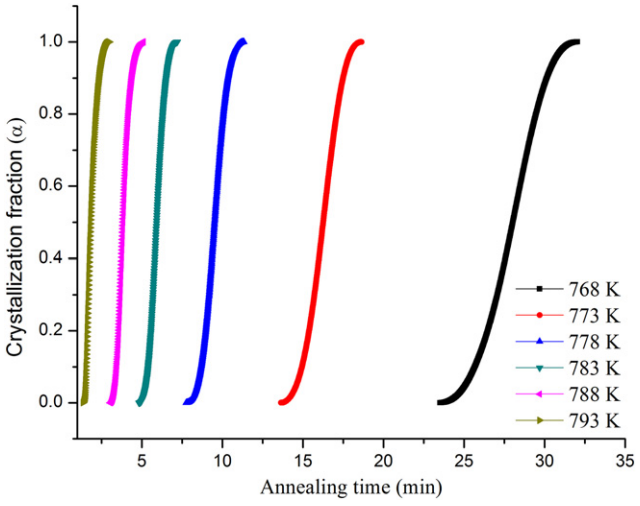

Fig. 6. Relationship between crystallization fraction (α) and annealing time at different annealing temperatures.

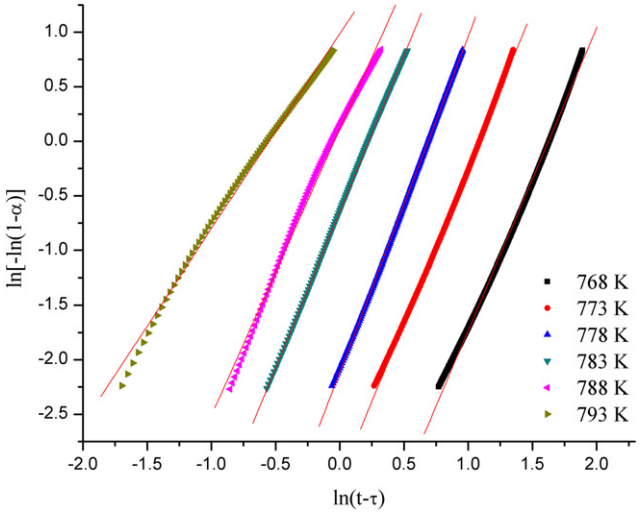

Fig. 7. JMA plots for the $Cu_{55}Hf_{45}$ glassy alloy.

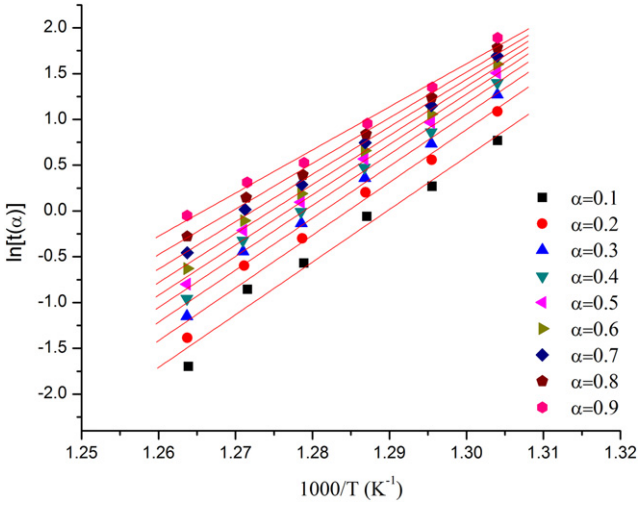

Fig. 8. Determination of the activation energy as a function of the different crystalline volume fractions, α, for the $Cu_{55}Hf_{45}$ glassy alloy.

phenomena is related to surface nucleation, one dimensional growth from surface to inside [30].

The activation energy for the crystallization process in the isothermal model can also be deduced by the Arrhenius equation using the relation between the time required, $t(\alpha)$, for a given crystallized fraction, α, and the annealing temperature [20]:

$$t(\alpha) = t_0 \exp\left[\frac{E_c(x)}{RT}\right] \quad (5)$$

where t_0 is a constant. Fig. 8 shows the approximate straight lines obtained by fitting the experimental values using Arrhenius equation as a function of crystalline volume fractions ($\alpha = 0.1, 0.2, 0.3, 0.4, 0.5, 0.6, 0.7, 0.8$ and 0.9) According to Eq. (5) the activation energy can be obtained from the slope of the fitted straight lines. The average value was 447.92 ± 16.1 kJ/mol for isothermal heating condition. This value of the activation energy, by isothermal heating, is very close to that determined from the non-isothermal heating by Kissinger analysis (444.73 ± 14.2 kJ/mol), this implies that the crystallization phenomena on isothermal and non-isothermal heating follows a very similar phase transformation mechanism [31].

In Fig. 9 the activation energy as a function of crystallization volume fraction, α, is presented. During isothermal analysis, the activation energy can determine how easy the crystallization proceeds. Here, it can be observed that the activation energy decreases as the magnitude of α increases. This behavior could be explained in terms of the activation energy, since it consists of two main components: nucleation and grain growth: when the crystallization progress takes place, the energy required for nucleation decreases, therefore, the total value of the activation energy is lower. On the other hand, at an initial stage, the magnitude of the activation energy suggested the presence of a high-energy barrier for crystallization. As the crystallization progresses, the activation energy drops rather fast (from 480 ± 24 kJ/mol to 391 ± 19.55 kJ/mol) implying that the crystallization phenomena follows semi-lineal behavior ($R^2 = 0.9368$) as a function of the crystallized fraction (between $0.1 \le \alpha \le 0.9$)

Table 2
Kinetic parameters for the $Cu_{55}Hf_{45}$ glassy alloy.

Annealing temperature (K)	Incubation time, τ (min)	Avrami exponent, n	Reaction rate constant, K
768	23.52 ± 0.16	2.78	0.20 ± 0.01
773	13.64 ± 0.15	2.87	0.34 ± 0.02
778	7.75 ± 0.17	3.07	0.50 ± 0.02
783	4.82 ± 0.13	2.86	0.80 ± 0.04
788	3.03 ± 0.15	2.65	1.04 ± 0.05
793	1.35 ± 0.09	1.79	1.74 ± 0.09

4. Conclusions

By means of differential scanning calorimetry, the crystallization kinetics of $Cu_{55}Hf_{45}$ was investigated in non-isothermal and isothermal conditions. In non-isothermal condition, the activation energies were determinate according to Kissinger's equation. The obtained values of E_g, E_x and E_p were 700.8 ± 20.3 kJ/mol, 469.4 kJ ± 12.7/mol and 444.73 ± 14.2 kJ/mol, respectively, while under isothermal process the E_a value was 447.92 ± 16.1 kJ/mol. A good agreement between these conditions was found. In isothermal conditions, the average value of calculated Avrami exponent was $n = 2.7$. These values assume that the crystallization mechanism implies a volume nucleation and two-dimensional growth. The local activation energy decreased as a function of the increment of the crystallization volume. This could be related to the crystallization progresses, as the energy required for nucleation drops when the crystallization fraction increases.

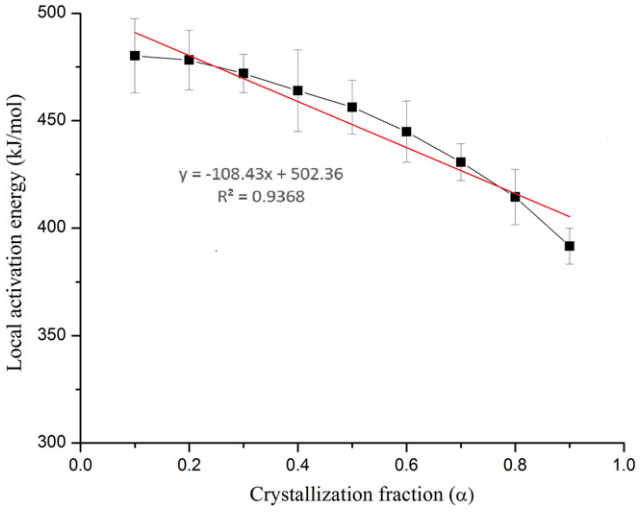

Fig. 9. Activation energy as a function of crystallization volume fraction, α, for $Cu_{55}Hf_{45}$ glassy alloy.

Acknowledgements

The authors are grateful for the financial support of UNAM-DGAPA-PAPIIT through grant no. IN101016. A. Tejeda, O. Novelo, F. García, A. López-Vivas, C. Flores Morales and C. Ramos are also acknowledged for their valuable technical support. “Por mi raza hablará el espíritu”.

References

[1] W. Klement, R.H. Willens, P. Duwez, Non-crystalline structure in solidified gold silicon alloys, Nature 187 (1960) 869–870.
[2] S. Kavesh, J.J. Gillman, H.L. Leamy, Metallic Glasses, ASM International, Metals Park, 1978.
[3] T. Masumoto, R. Maddin, The mechanical properties of palladium 20 a/o silicon alloy quenched from the liquid state, Acta Metall. 19 (7) (1971) 725–741.
[4] H.J. Fetch, J.H. Perepezco, M.C. Lee, W.L. Johnson, Thermodynamic properties and crystallization kinetics of glass-forming undercooled liquid Au-Pb-Sb alloys, J. Appl. Phys. 68 (9) (1990) 4494–4502.
[5] F.X. Qin, K. Wada, X.J. Yang, X.M. Wang, M. Yoshimura, K. Asami, A. Inoue, Bioactivity of a Ni-free Ti-based metallic glass, Mater. Trans. 51 (3) (2010) 529–534.
[6] A. Inoue, T. Zhang, T. Masumoto, Glass-forming ability of alloys, J. Non-Cryst. Solids 156-158 (2) (1993) 473–480.
[7] F.Q. Guo, S.J. Poon, G.J. Shiflet, CaAl-based bulk metallic glasses with high thermal stability, Appl. Phys. Lett. 84 (1) (2004) 37–39.
[8] G. Duan, D. Xu, W.L. Johnson, High copper content bulk glass formation in bimetallic Cu-Hf system, Metall. Mater. Trans. A 36 (2005) 455–458.
[9] L. Xia, W.H. Li, S.S. Fang, B.C. Wei, Y.D. Dong, Binary Ni-Nb bulk metallic glasses, J. Appl. Phys. 99 (2006) 026103.
[10] A. Inoue, W. Zhang, Formation, thermal stability and mechanical properties of Cu-Zr and Cu-Hf binary glassy alloy rods, Mater. Trans. 45 (2) (2004) 584–587.
[11] A. Pratap, K.N. Lad, T.L.S. Rao, P. Majmudar, N.S. Saxena, Kinetics of crystallization of amorphous $Cu_{50}Ti_{50}$ alloy, J. Non-Cryst. Solids 345&346 (2004) 178–181.
[12] S.T. Shan, L. Xia, D. Ding, Y.D. Dong, Thermal stability and kinetics of binary $Cu_{65}Hf_{35}$ bulk metallic glass, Chin. Phys. Lett. 23 (11) (2006).
[13] L. Xia, D. Ding, S.T. Shan, Y.D. Dong, The glass forming ability of Cu-rich Cu-Hf binary alloys, J. Phys. Condens. Matter 18 (2006) 3543–3548.
[14] I.A. Figueroa, J.D. Plummer, G.A. Lara-Rodriguez, O. Novelo-Peralta, I. Todd, Metallic glass formation in the binary Cu–Hf system, J. Mater. Sci. 48 (2013) 1819–1825.
[15] P. Jia, J. Xu, Comparison of bulk metallic glass formation between Cu-Hf binary and Cu-Hf-Al ternary alloys, J. Mater. Res. 24 (1) (2008) 96–106.
[16] C.E. Borja-Soto, I.A. Figueroa, J.R. Fonseca, G.A. Lara-Rodriguez, J.A. Verduzco, Composition, elastic property and packing efficiency predictions for bulk metallic glasses in binary, ternary and quaternary systems, Mater. Res. 19 (2) (2016) 285–294.
[17] I. Kalay, M.J. Kramer, R.E. Napolitano, Crystallization kinetics and phase transformation mechanisms in $Cu_{56}Zr_{44}$ glassy alloy, Metall. Mater. Trans. A 46 (A) (2015) 3356–3364.
[18] Q. Gao, Z. Jian, J. Xu, M. Zhu, F. Chang, A. Han, Crystallization kinetics of the $Cu_{50}Zr_{50}$ metallic glass under isothermal conditions, J. Solid State Chem. 244 (2016) 116–119.
[19] H.E. Kissinger, Reaction kinetics in differential thermal analysis, Anal. Chem. 29 (1957) 1702–1706.
[20] M. Avrami, Kinetics of phase change I. General theory, J. Chem. Phys. 7 (1939) 1103–1112.
[21] E. Matsubara, T. Ichitsubo, K. Itoh, T. Fukunaga, J. Saida, N. Nishiyama, H. Kato, A. Inoue, Heating rate dependence of T_g and T_x in Zr-based BMGs with characteristic structures, J. Alloys Compd. 483 (2009) 8–13.
[22] H.E. Kissinger, Variation of peak temperature with heating rate in differential thermal analysis, J. Res. Natl. Bur. Stand. 57 (4) (1956) 217–221.
[23] R. Busch, Y.J. Kim, W.L. Johnson, Thermodynamics and kinetics of the undercooled liquid and the glasss transition of the $Zr_{41.2}Ti_{13.8}Cu_{12.5}Ni10Be_{22.5}$ alloy, J. Appl. Phys. 77 (8) (1994) 4039–4043.
[24] H.R. Wang, Y.L. Gao, G.H. Min, X.D. Hui, Y.F. Ye, Primary crystallization in rapidly solidified $Zr_{70}Cu_{20}Ni_{10}$ alloy from supercooled liquid region, Phys. Lett. A 314 (2003) 81–87.
[25] L.C. Chen, F. Speapen, Calorimetric evidence for the quasicrystalline structure of 'amorphous' Al/transition metal alloys, Nature 336 (1988) 366–368.
[26] C.S. Ray, W.H. Huang, D.E. Day, Crystallization kinetics of a Lithia–silica glass: effect of sample characteristics and thermal analysis measurement techniques, J. Am. Ceram. Soc. 74 (1) (1991) 60–66.
[27] W.A. Johnson, R.F. Mehl, Reaction kinetics in processes of nucleation and growth, Trans. Am. Inst. Min. Metall. Pet. Eng. 135 (1939) 416–422.
[28] J.Z. Jiang, Y.X. Zhuang, H. Rasmussen, Formation of quasicrystals and amorphous-to-quasicrystalline phase transformation kinetics in $Zr_{65}Al_{7.5}Ni_{10}Cu_{7.5}Ag_{10}$ metallic glass under pressure, Phys. Rev. B (2001) 64.
[29] S. Mahadevan, A. Giridhar, A.K. Singh, Calorimetric measurements on As-Sb-Se glasses, J. Non-Cryst. Solids 88 (1) (1986) 11–34.
[30] J.W. Christian, The Theory of Transformation in Metals and Alloys, Pergamon Press, Oxford, 1965.
[31] Y.D. Sun, P. Shen, Z.Q. Li, J.S. Liu, M.Q. Cong, M. Jiang, Kinetics of crystallization process of Mg-Cu-Gd based bulk metallic glasses, J. Non-Cryst. Solids 358 (2012) 1120–1127.